Electronic Supplementary Material (ESI) for Lab on a Chip.
This journal is © The Royal Society of Chemistry 2016

Electronic Supplementary Information

Magnetic separation of microparticles by shape

Ran Zhou, Feng Bai, and Cheng Wang*

Department of Mechanical and Aerospace Engineering, Missouri University of Science and Technology, 400 W. 13th St., Rolla, Missouri, 65409, United States

1. Preparation of ellipsoidal magnetic microparticles

Ellipsoidal microparticles were prepared from monodisperse spherical polystyrene particles following the approaches of Ho et al.[1] Spherical magnetic particles used in this work were magnetite-doped and un-cross-linked polystyrene microspheres, and were purchased from Micromod GmbH, Germany. The mean diameter of the spherical magnetic particles is d = 7 μm (coefficient of variation < 5%), and its density is 1.1 g/mL.

To prepare the ellipsoidal particles, first, the particles were embedded in a PVA film. In this step, 4 g of polyvinyl alcohol (PVA) was dissolved in 120 g distilled water of 85 degrees Celsius to obtain the aqueous polyvinyl alcohol (PVA) solution. The homogenous PVA solution was obtained by mechanical stirring with a compact digital mixer (Cole-Parmer, USA) at a speed of 600 rpm for 60 mins. Next, 0.4 mL of the original spherical magnetic particles suspension containing 5% (w/w) particles was added to the PVA solution and stirred at a speed less than 300 rpm to avoid foaming. The homogeneous PVA-particle suspension was then degassed, and cast onto a flat plastic tray (7” × 5” × 0.5”). A particle-embedded PVA film was formed after 2 days due to natural evaporation at room temperature.

Second, the film was cut into small 2” × 3” pieces and stretched using a custom-designed mechanical stretching device. The ends of the PVA-particle film were securely clamped on the moving blocks of the stretching device. Then, the film was immersed in an oil bath of 140 °C, and stretched uniformly to a pre-set length for 10 mins. During this process, the spherical particles in the film underwent a plastic deformation to ellipsoids.

At last, the film was subsequently removed from the oil bath and cooled to room temperature, and the particles were recovered by dissolving the PVA matrix. In this step, the PVA-particle film was cooled and cleaned with isopropyl alcohol (IPA) to remove oil from the film surfaces. Subsequently, the edges of the stretched film were cut off, and only the central part was selected for further processing because of non-uniform stretching of the film near the clamps. And then, the central part was cut into small pieces of approximately 1 cm × 1 cm, and soaked in 30% (v/v) aqueous IPA while being stirred for 1-2 h to remove any traces of oil. The IPA solution was decanted and replaced with fresh IPA solution. The film was then heated to 85 °C for 1 h to dissolve the PVA matrix thoroughly. After that, the dispersion was centrifuged at 3300 rpm for

[1] Ho, C. C., et al. "Preparation of monodisperse ellipsoidal polystyrene particles." Colloid and Polymer Science 271.5 (1993): 469-479.

30 mins to sediment the particles, and the clear high viscous PVA-rich supernatant at the top was poured off. The same washing procedure was repeated five more times. Some large impurities were then excluded from the solution with nylon filter screen of 38 μm opening size (Prod No. 41-6140, Ted Pella, Inc., USA). The filtered dispersion was centrifuged again and the supernatant at the top was poured off. The ellipsoidal particles were obtained, and re-dispersed distilled water.

A representative micrograph of the particles obtained from this method is shown in Fig. S1 (a). The corresponding probability density function (PDF) of the aspect ratio r_p in Fig. S1 (b) shows that mean aspect ratio is $\overline{r_p} = 3.93$ and the standard deviation is $\sigma_p = 0.43$, illustrating that most ellipsoids in our study has a uniform shape.

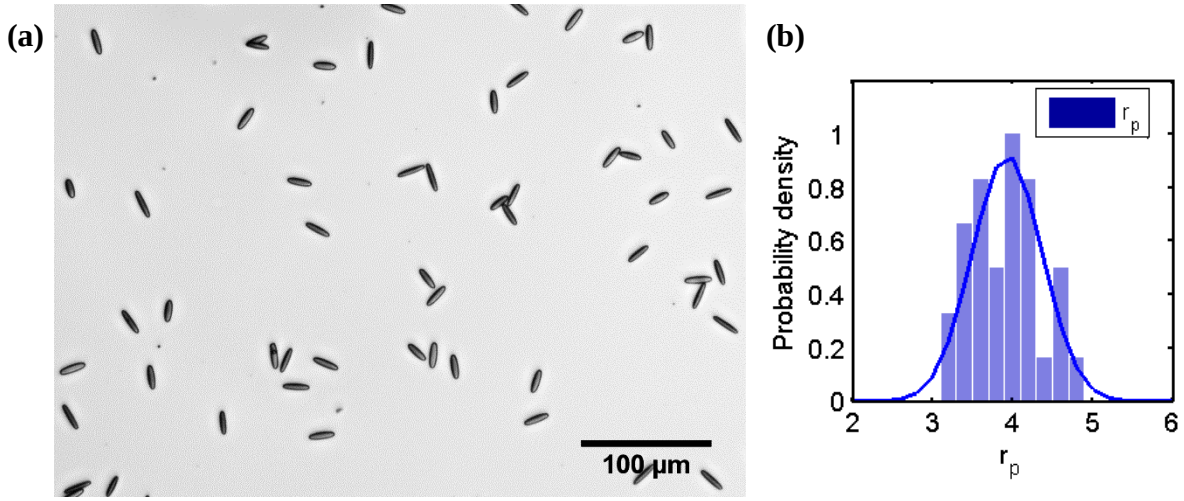

Figure S1. (a) Micrograph of magnetic ellipsoidal particles with mean aspect ratio of $\overline{r_p} = 3.93$, obtained starting from 7 μm spheres. (b) Probability density function (PDF) of the aspect ratio r_p.

2. Uniform magnetic field generated by Halbach array from identical bar magnets

A Halbach array is a special arrangement of permanent magnets that augments the magnetic field on one side of the array while cancelling the field to near zero on the other side[2]. This is achieved by having a spatially rotating pattern of magnetization. The Halbach cylinder is a special and useful pattern of Halbach array. It is a magnetized cylinder composed of ferromagnetic material, and intense magnetic field confined entirely within the cylinder with zero field outside. The flux on the surface of a cylinder or circle containing an homogeneous field, is given by the polar coordinates[3]

[2] Halbach, Klaus. "Design of permanent multipole magnets with oriented rare earth cobalt material." Nuclear instruments and methods 169.1 (1980): 1-10.

[3] Raich, H., and Peter Blümler. "Design and construction of a dipolar Halbach array with a homogeneous field from identical bar magnets: NMR Mandhalas." Concepts in Magnetic Resonance Part B: Magnetic Resonance Engineering 23.1 (2004): 16-25.

$$M := \begin{pmatrix} M_t \\ M_n \end{pmatrix} = M_0 \begin{pmatrix} sin\theta \\ cos\theta \end{pmatrix} \quad with\ \theta = 0 \dots 2\pi \qquad (1)$$

with M_t the tangential and M_n the normal component in Fig. S2[3] (a).

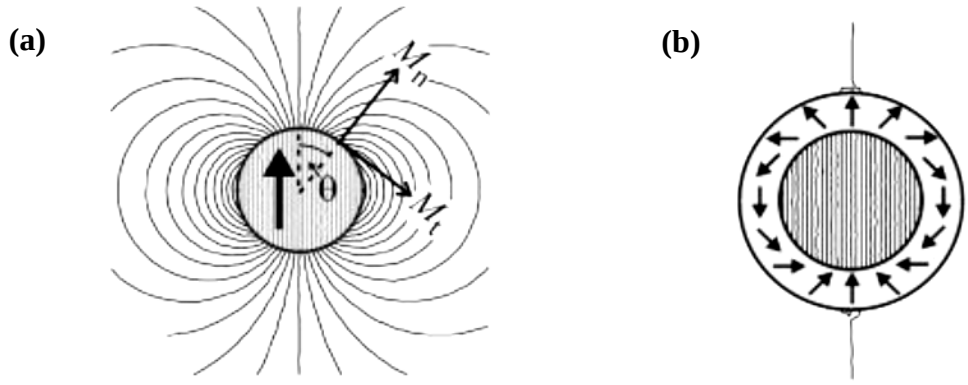

Figure S2 Explanation of the Halbach geometry according to Eqs. (1) and (2): (a) Magnetic flux inside and around a homogeneously magnetized cylinder. The axes illustrate the normal, M_n, and tangential, M_t, magnetization directions. (b) The field of a dipolar Halbach array with flux inside. Arrows indicate the magnetization direction[3].

Discrete magnetic parts, e.g. permanent magnets, can be used to mimic these field characteristics inside a hollow cylinder as presented in Fig. S3, and the magnetization direction in the i^{th} magnet has to be[4]

$$\gamma_i := (1 + k)\beta_i$$
$$with\ k \in \mathbb{Z}\ \ and\ i = 0, 1, \dots, n-1 \qquad (2)$$

where k is the number of pole-pairs or modes; $\beta_i = \left(\frac{360}{n}\right) i$, and n is the number of permanent magnets. As displayed in Fig. S2[3] (b), for the envisaged concept of homogeneous flux inside the magnet ring, $k = 1$. Such arrays are also known as "magic rings" [5,6,7].

In our study, the Halbach array generating uniform magnetic field consisted of twenty cuboid 0.25" × 0.25" × 0.5" permanent magnets (K&J Magnetics, Inc.) that were fixed in a plastic holder fabricated by 3D printing technique, as shown in Fig. S3. The magnitude of the magnetic field within the central region is $H_0 \approx 35000\ A/m$, as measured by a Gaussmeter. Table S1 summarizes the placement angle of each magnet within this Halbach array, where i, β_i and

[4] Zhu, Z. Q., and D. Howe. "Halbach permanent magnet machines and applications: a review." IEE Proceedings-Electric Power Applications 148.4 (2001): 299-308.

[5] Leupold, Herbert A., Anup S. Tilak, and Ernest Potenziani II. "Multi-Tesla permanent magnet field sources." Journal of applied physics 73.10 (1993): 6861-6863.

[6] Leupold, Herbert A., E. Potenziani, and A. S. Tilak. "Adjustable multi-tesla permanent magnet field sources." IEEE transactions on magnetics 29.6 (1993): 2902-2904.c

[7] Abele, M. G., et al. "Compensation of non-uniform magnetic properties of components of a yokeless permanent magnet." IEEE Transactions on Magnetics 25.5 (1989): 3904-3906.

γ_i can be referred in Eq. (2) and Fig. S3. According to the design in Table S1, a uniform magnetic field can be generated inside the Halbach cylinder, as mentioned in Fig. S2[3] (b).

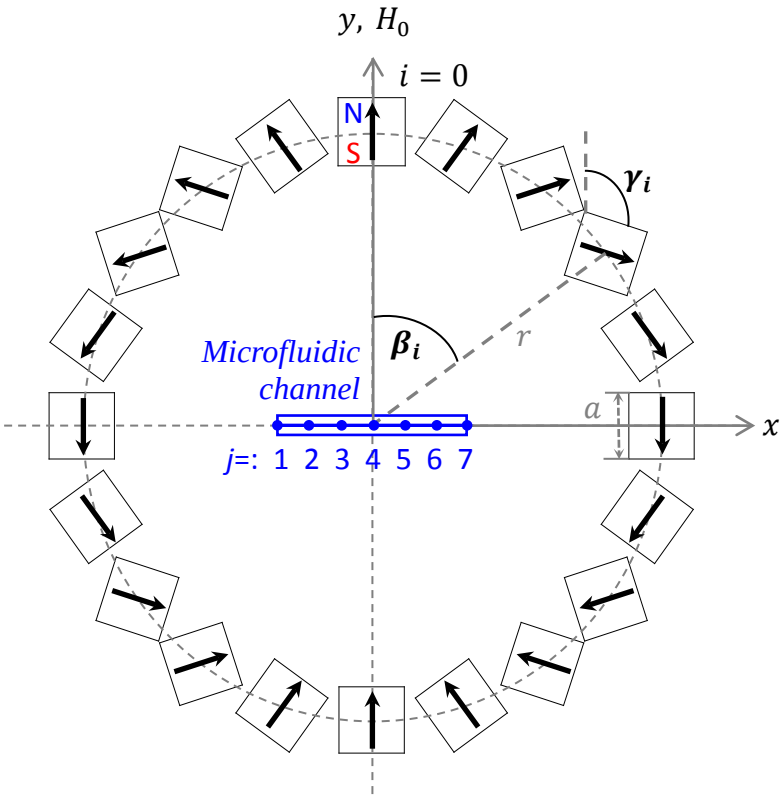

Figure S3 Schematic geometry of Halbach cylinder assembled by twenty bar magnets. The bottom of each bar magnet is a square with the side length of a=0.25 inch; the radius of Halbach cylinder is r=2.5 cm; β_i and γ_i are illustrated in Eq. (2).

Table S1 Placement angles of permanent magnets within a Halbach cylinder.

i	β_i(°)	γ_i(°)
0	0	0
1	18	36
2	36	72
3	54	108
4	72	144
5	90	180
6	108	216
7	126	252
8	144	288
9	162	324
10	180	360

11	198	396
12	216	432
13	234	468
14	252	504
15	270	540
16	288	576
17	306	612
18	324	648
19	342	684

Furthermore, Table S2 and Fig. S4 present the experimental measurement of the magnetic field strength H_0 within the range of the microfluidic channel in Fig. S3. Accordingly, the magnetic field can be reasonably regarded as a uniform one within the range of the microfluidic channel.

Table S2 Experimental measurement of magnetic field strength H_0 corresponding to different positions within the microfluidic channel in Fig. S3.

Position No. j	H_{0_j} (A/m)
1	35411.97
2	35809.86
3	34695.78
4	34854.93
5	35173.24
6	35014.09
7	35411.97
Mean H_0	**35195.98**

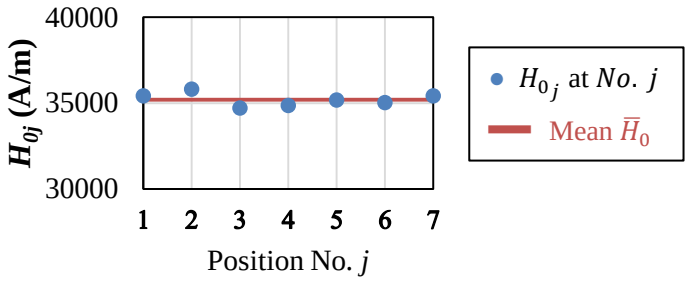

Figure S4 Experimental measurement of magnetic field strength H_0 at different postions in Fig. S3 and Table S2.

3. Lateral migration and separation of nonmagnetic particles

The shape-dependent lateral separation takes place as long as the suspended non-spherical particles and the surrounding fluid have different magnetic susceptibilities: paramagnetic particles suspended in a nonmagnetic fluid, or nonmagnetic particles suspended in a magnetic fluid (e.g. ferrofluid EMG 408), as shown in Fig. S5. This is because magnetic torques will arise due to the susceptibility contrast [8]; and similar asymmetrical particle rotation and lateral migration will result.

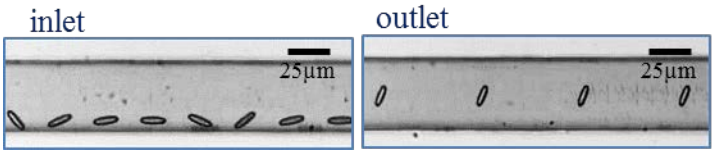

Figure S5 Trajectories of individual nonmagnetic particles in a ferrofluid at the inlet and outlet respectively. The flow rates were Q1 = 1.0 μL/min and Q2 = 0.2 μL/min.

4. Lift mechanism of ellipsoidal particles

The asymmetric rotation of the particles, coupled with hydrodynamic interactions with the wall, causes a non-zero net lift force. The hydrodynamic interactions refer to the coupling of rotational and translation motions due to the presence of the wall. In unbounded Stokes flows, the rotation and translation of an ellipsoidal particle are decoupled[9]: the translation can be determined from the force acting on the particle and the translation mobility tensor, while the rotation can be determined from the torque and the rotation tensor. The particle rotation in unbounded flows will not induce translational motions, if there the total force on the particle is zero.

The proximity of a wall will induce a coupling between the translation and rotation. For example, the rotation of an ellipsoidal particle near a wall will generally result in a force (i.e. translation). This is illustrated with an ellipsoidal particle in a simple shear flow, in Figure S6. The hydrodynamic interactions (or coupling) cause periodical lateral motions towards and away from the wall. The particle will have a zero net lateral migration (or zero net lift force) over one period. There are analytical solutions for the coupling of the rotation and translation for spherical particles near a wall[9]. However, for ellipsoidal particles, the coupling depends on both the separation distance between the particle and the wall, as well as the orientation angle of the particle. These difficulties have prevented the finding of analytical solutions. The hydrodynamic interactions have been investigated with numerical simulations in the literature[10,11,12].

---

[8] Stratton JA. "Electromagnetic Theory". Adams Press; 2007.

[9] Happel J, Brenner H. Low Reynolds Number Hydrodynamics. Englewood Cliffs NJ 1983.

[10] Feng J, Joseph DD. The unsteady motion of solid bodies in creeping flows. J. Fluid Mech. 1995;303(1):83.

[11] Gavze E, Shapiro M. Particles in a shear flow near a solid wall: Effect of nonsphericity on forces and velocities. Int. J. Multiph. Flow 1997;23(1):155-182.

[12] Gavze E, Shapiro M. Motion of inertial spheroidal particles in a shear flow near a solid wall with special application to aerosol transport in microgravity. J. Fluid Mech. 1998;371:59-79.

When a uniform magnetic field is applied, the magnetic torque breaks the symmetry of the rotational angular velocities of the particle. This asymmetry in turn breaks the symmetry of the lateral oscillatory motions of the particles, leading to a non-zero net lateral migration. In our study, the observed lateral migration of the ellipsoidal particles was thus due to three essential elements: the non-spherical shape, magnetic torque, and proximity of a channel wall.

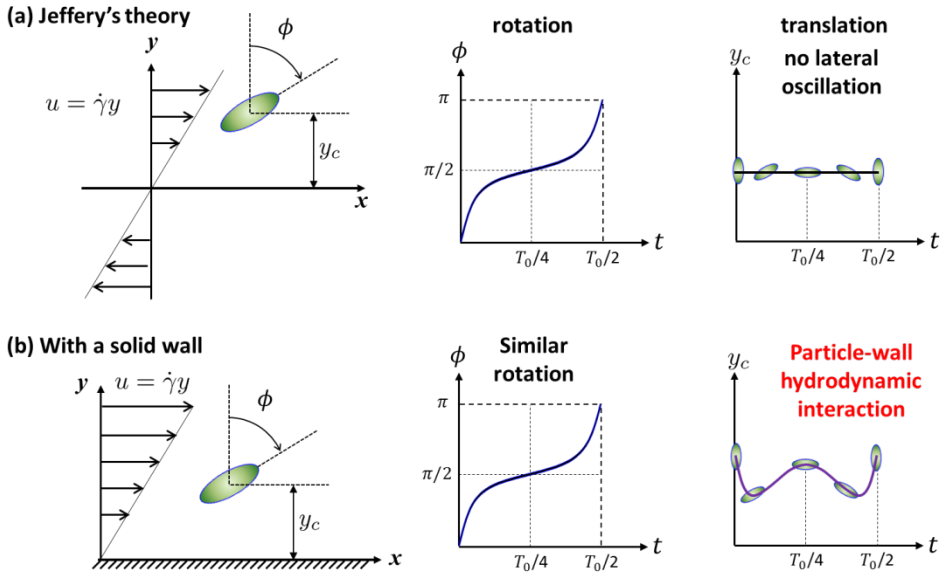

Figure S6. Illustration of the rotational and translational motions of an ellipsoidal particle in a simple shear flow. (a) Jeffery's model in an unbounded flow, and (b) influence of a wall.